ISBN: 978-3-95450-132-8 doi:10.18429/JACoW-IPAC2014-TUPRI048

# A MAP APPROACH FOR ELECTRON CLOUD DENSITY IN A STRONG LHC DIPOLE

W. Di Carmine, S. Petracca*, A. Stabile, University of Sannio, Benevento, and INFN, Salerno, Italy

*Abstract*

The evolution of the electron density during electron cloud formation can be reproduced using a bunch-to-bunch iterative map formalism. The reliability of this formalism has been proved for RHIC [1] and LHC [2]. A formula for the linear coefficient has been already found [2]. Here we derive an analytic expression for the quadratic map coefficient in the LHC strong magnetic dipole and compare with simulations results.

## INTRODUCTION

Most studies performed so far were based on computer simulations (ECLOUD [3]) yielding a very detailed description of the electron cloud evolution. In [2,4,5] it was shown that, for the typical parameters of the LHC, the evolution of the transverse electron cloud density from bunch to bunch can be described by a simple cubic map:

$$\lambda_{m+1} \;=\; a\,\lambda_m + b\,{\lambda_m}^2 + c\,{\lambda_m}^3 \tag{1}$$

where $\lambda_m$ is the average cloud density of electrons after the $m$-th passage of the bunch. The coefficients $a$, $b$, $c$ are extrapolated from simulations, and are functions of the beam parameters and of the beam pipe features. The linear term describes the linear growth and the coefficient $a$ is larger than unity in the presence of electron cloud formation. The quadratic term describes the space charge effects, and is negative reflecting the concavity of the curve $\lambda_{m+1}$ vs $\lambda_m$. The cubic term, $c$, corresponds to a variety of subtler effects, acting as perturbations to the above simple scenario.

In this paper we generalize our results in [5] and derive an analytical expression for the quadratic coefficient $b$, under the simple assumptions of a round chamber and in the presence of a uniform magnetic field with reference to the LHC (Table 1). The coefficient $b$ turns out to be dependent on few beam and machine parameters, and can be computed analytically once for all.

Table 1: LHC Input Parameters

| Parameters | Quantities | Unit | Value |
|---|---|---|---|
| Beam pipe radius (circ.) | $R_p$ | m | 0.020 |
| Beam size | $\sigma_r$ | m | 0.002 |
| Bunch spacing | $s_b$ | m | 7.480 |
| Bunch length | $\sigma_z$ | m | 0.023 |
| Particles per bunch | $N_b$ | $10^{10}$ | $8 \div 12$ |
| Magnetic filed | $B$ | T | 8 |

* petracca@sa.infn.it

## THE SATURATION ELECTRON DENSITY

The average transverse electron density grows up exponentially in time until the space charge due to the electrons themselves produces a saturation level. Once the saturation level is reached the average electron density does not change significantly. The final decay corresponds to the empty interval between successive bunches (Fig. 1).

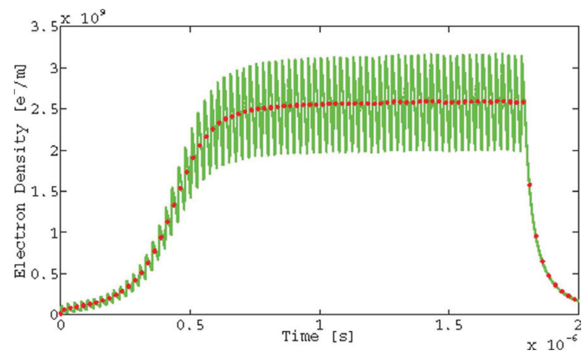


Figure 1: Time evolution of the (average transverse) electron density computed with PyCLOUD [6]. The points mark the average electron density between two consecutive bunches. The machine/beam parameters used are listed in Table 1.

The energy barrier seen by each electron coming from the pipe wall towards the center of the chamber, is given by:

$$\mathcal{E}(r,\phi) \;=\; -e\,V(r,\phi), \tag{2}$$

where $r \;=\; \sqrt{x^2+y^2}$, $\phi \;=\; \arctan(y/x)$ are the polar coordinates in the transverse $(x\;y)$ plane and $r$ is in units of the pipe radius $R_p$. The total electrostatic potential

$$V(r,\,\phi) = V_b(r,\,\phi) + V_{ec}(r,\,\phi) \tag{3}$$

due to the bunch and the e-cloud is computed from:

$$V_{ec}(r,\phi) = \int_{S'} dS'\,g(r',\,\phi')\,v(r,\phi,r',\phi') \tag{4}$$

$$V_b = -\frac{e\,\lambda_b}{2\,\pi\,\epsilon_0}\ln r\,\Theta(r-\tilde{\sigma}_r) \tag{5}$$

where $\Theta$ is the Heaviside function and $v(r,\phi,r',\phi')$ is the electrostatic potential generated by a negative uniform charge line density $(-e\,\lambda_e)$, located in $(r',\phi')$, satisfying the boundary conditions $v(1,\,\phi) \;=\; 0$ on the chamber wall:

$$v(r,\phi,r',\phi') = \frac{-e\lambda_e}{4\pi\epsilon_0}\ln\frac{r^2r'^2 - 2rr'\cos(\phi'-\phi)+1}{r^2-2rr'\cos(\phi'-\phi)+r'^2} \tag{6}$$

The choice of the function $g(r,\,\phi)$ is crucial. In fact $g(r,\,\phi)$ has to provide the two-dimensional distribution of the electron cloud in the saturation phase. In Fig. 2 we show the

ISBN: 978-3-95450-132-8 doi:10.18429/JACoW-IPAC2014-TUPRI048

output of simulation and, then, we formulate a distribution model,

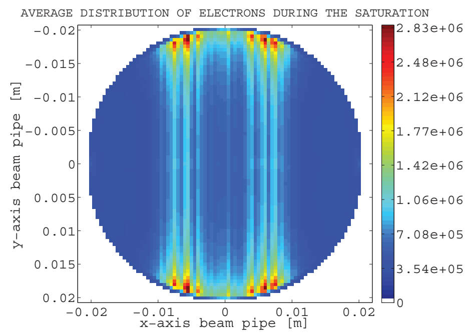


Figure 2: Snapshot of the space charge spatial distribution in the trasverse plane with SEY=1,5 and B=8T.

$$f(r,\phi) = X_p\left[e^{-\frac{(x-x_p)^2}{2\sigma_p{}^2}} + e^{-\frac{(x+x_p)^2}{2\sigma_p{}^2}}\right] + X_c\, e^{-\frac{x^2}{2\sigma_c{}^2}} + X_u \quad (7)$$

$$g(r,\phi) \;=\; \frac{f(r,\phi)}{\int_{S'} dS' f(r',\phi')} \quad (8)$$

where $x = r\cos\phi$ and $X_p, X_u, X_c, \sigma_p, \sigma_c$ are free parameters. In the absence of the magnetic field the electron cloud density has a circular distribution in the plane $x\,y$.

In Fig. 3 we compare the energy barrier in the presence and in the absence of the magnetic dipole field $\vec{B}$. The barrier inside the dipole is lower than in free space, assuming a radial distribution, with $\phi = \pi/2$.

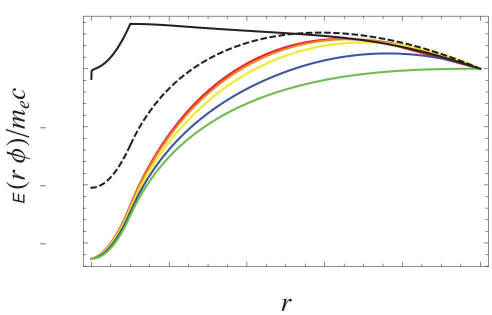


Figure 3: Plot of energy barrier inside the dipole for fixed values of angle $\phi = 0, \pi/8, \pi/4, 3\pi/8, \pi/2$ (colored lines from the top to the bottom). For $\vec{B} = 0$ we consider the uniform (black line) and the gausslike distribution of space charge (dashed line). In Eq. (8) we assume: $X_p = 2$, $x_p = 0.7$, $\sigma_p = 0.2$, $X_c = 0.5$, $\sigma_c = 0.1$, $\lambda_e = 10 * \bar{\lambda}_b = 10^{11}$.

## ANALYTICAL DETERMINATION OF LINEAR COEFFICIENT

The linear coefficient of the map (1) in a dipole magnet has been computed [2] as

$$a(E,\mathcal{E}_0) \;=\; \delta_r^k + \delta_{ts}\,\delta_{tot}{}^{\xi}\,\frac{\delta_{tot}{}^{k\,\xi} - \delta_r{}^k}{\delta_{tot}{}^{\xi} - \delta_r} \quad (9)$$

where $k$ is the total number of collisions with the pipe wall made by electrons with energy $E_g$ during the interval preceding the passage of the next bunch and $\xi = \sqrt{\mathcal{E}_0/E_g} \ll 1$. The adopted SEY model is given by the following expressions [7]:

$$\begin{aligned}
\delta_{ts}(E) &= \delta_{max}\frac{s(E/E_{max})}{s-1+(E/E_{max})^s}\\
\delta_r(E) &= R_0\left(\frac{\sqrt{E}-\sqrt{E+E_0}}{\sqrt{E}+\sqrt{E+E_0}}\right)^2 \quad (10)\\
\delta_{tot}(E) &= \delta_{ts}(E)+\delta_r(E)
\end{aligned}$$

where $\delta_{max} = \delta_{ts}(E_{max})$. The other parameters are summarized in Table 2.

Table 2: Values of SEY Parameters (Eq. 10)

| Parameters | Quantities | Unit | Value |
|---|---|---|---|
| Maximum SEY | $\delta_{max}$ | / | 1.5 ÷ 1.7 |
| Energy for max $\delta$ | $E_{max}$ | eV | 332 |
| - | $s$ | / | 1.35 |
| - | $E_0$ | eV | 150 |
| - | $R_0$ | / | 0.7 |

The SEY also depends on the angle at which the electrons strike the chamber wall. From fitting of the experimental data one has $\delta_{max}(\theta) = \delta_{max}\exp((1-\cos\theta)/2)$ and $E_{max}(\theta) = E_{max}(1 + 0.7 * (1-\cos\theta))$.

## ANALYTICAL DETERMINATION OF QUADRATIC COEFFICIENT

The coefficient $b$ is found by imposing the condition of saturation $\lambda_{m+1} = \lambda_m = \lambda^{sat}$ in the map (1), and neglecting the cubic term. Using the more general expression (9) we accordingly obtain

$$b \;=\; b(E,\mathcal{E}_0) \;=\; \frac{1-a(E,\mathcal{E}_0)}{\lambda_e^{sat}} \quad (11)$$

The saturation density can be obtained by imposing that at some points $(\bar{r},\bar{\phi})$ of the trasverse plane $(x,y)$ the electron energy $\mathcal{E}_0$ satisfies the condition $\mathcal{E}(\bar{r},\bar{\phi}) \geq \mathcal{E}_0$ [8].

We can rewrite equation (2) as:

$$\mathcal{E}(r,\phi) = 2r_e m_e c^2(\lambda_e h_e(r,\phi) - \lambda_b h_b(r)), \quad (12)$$

to get:

$$\lambda_e(r,\phi,\mathcal{E}(r,\phi)) = \frac{\mathcal{E}(r,\phi)}{2r_e\, m_e c^2\, h_e(r,\phi)} + \lambda_b\frac{h_b(r)}{h_e(r,\phi)}. \quad (13)$$

ISBN: 978-3-95450-132-8 doi:10.18429/JACoW-IPAC2014-TUPRI048



At saturation the transverse motion of electrons is approximately vertical ($x = const$) inside the dipole. Therefore

$$\bar{r}(x) = \sqrt{x^2 + (1-x^2)(\Gamma-1)^2}$$
$$\bar{\phi}(x) = \arctan\left(\frac{\sqrt{1-x^2}(\Gamma-1)}{x}\right) \tag{14}$$

where $\Gamma = (s_b/R_p)\sqrt{2\mathcal{E}_0/m_e c^2} \sim 1.65$ for LHC (see Table 1), and we can compute the saturation density as

$$\lambda_e^{sat} = \int_{S'} dS' g(x',y') \lambda_e\left(\bar{r}(x'), \bar{\phi}(x'), \mathcal{E}_0(1-x'^2)\right) \tag{15}$$
$$\lambda_e^{sat} \sim \lambda_e\left(\bar{r}(x_p), \bar{\phi}(x_p), \mathcal{E}_0(1-{x_p}^2)\right)$$

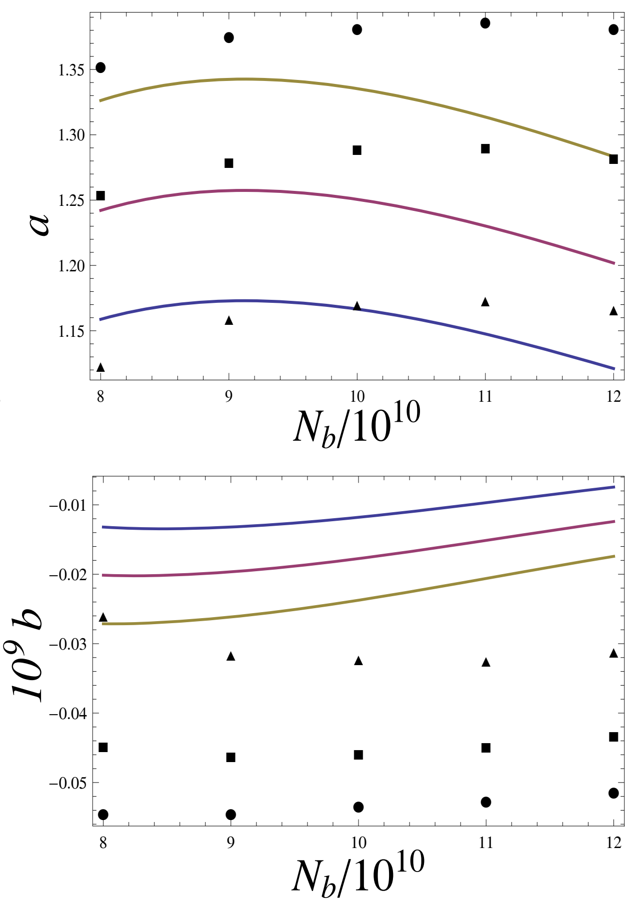


Figure 4: Comparison between mapping and simulations results for the coefficient $a$ and $b$ (16) by setting $\delta_{max} = 1.5$ (blue line and triangles), 1.6 (black line and squares), 1.7 (yellow line and circles). The values of density parameters are $X = 1$, $X_p = 0.4$, $\sigma_p = 0.2$, $X_c = 0$, $X_u = 0.3$.

The coefficients $a$ and $b$ of the quadratic map are thus given by

$$a = a(E_g, \mathcal{E}_0(1-{x_p}^2))$$
$$b = \frac{1-a(E_g, \mathcal{E}_0(1-{x_p}^2))}{\lambda_e\left(\bar{r}(x_p), \bar{\phi}(x_p), \mathcal{E}_0(1-{x_p}^2)\right)} \tag{16}$$

where $E_g$ is the energy gain of the accelerated electron after the passage of the bunch. In Fig. 4 we show the comparison between our model and the PyCloud simulations for the coefficients $a$ and $b$ in the presence of a magnetic dipole field.

## CONCLUSIONS

A simple analytic form for the quadratic map coefficient has been derived in the presence of a uniform magnetic field, and found to be in good agreement with the results obtained from PyCLOUD simulations. The map formalism can thus be easily applied to determine safe regions in parameter space where the electron clouds effects are reduced.

## REFERENCES


[1] U.Iriso and S.Peggs, "Maps for Electron Clouds", Phys.Rev. ST-AB8, 024403, 2005.

[2] T.Demma et al., "Maps for Electron Clouds: Application To LHC", Phys.Rev.ST-AB10, 114401 (2007).

[3] F. Zimmermann, "A Simulation Study of Electron-Cloud Instability and Beam-Induced Multipacting in the LHC", CERN LHC-Project-Rept. 95 (1997).

[4] Th. Demma et al., "Maps for Electron Cloud Density in Large Hadron Collider Dipoles", Phys. Rev. ST-AB **10** (2007) 114401.

[5] Th. Demma et al., "E-Cloud Map Formalism: an Analytical Expression for Quadratic Coefficient", Proc. IPAC'10, Kyoto, Japan, May 23-28 2010.

[6] G. Iadarola, G. Rumolo, CERN Yellow Rep. 2013-002 189

[7] M. Furman, M. Pivi, "Probabilistic Model for the Simulation of Secondary Electron Emission", Phys. Rev. ST-AB **5** (2002) 12404.

[8] S. Heifets, "Electron Cloud at High Beam Currents", SLAC-PUB-9584 (2002).